Power Law Stretching of Associating Polymers in Steady-State Extensional Flow

Charley Schaefer* and Tom C. B. McLeish
Department of Physics, University of York, Heslington, York YO10 5DD, United Kingdom

(Received 23 October 2020; revised 2 December 2020; accepted 7 January 2021; published 2 February 2021)

We present a tube model for the Brownian dynamics of associating polymers in extensional flow. In linear response, the model confirms the analytical predictions for the sticky diffusivity by Leibler-Rubinstein-Colby theory. Although a single-mode Doi-Edwards-Marrucci-Grizzuti approximation accurately describes the transient stretching of the polymers above a "sticky" Weissenberg number (product of the strain rate with the sticky-Rouse time), the preaveraged model fails to capture a remarkable development of a power law distribution of stretch in steady-state extensional flow: while the mean stretch is finite, the fluctuations in stretch may diverge. We present an analytical model that shows how strong stochastic forcing drives the long tail of the distribution, gives rise to rare events of reaching a threshold stretch, and constitutes a framework within which nucleation rates of flow-induced crystallization may be understood in systems of associating polymers under flow. The model also exemplifies a wide class of driven systems possessing strong, and scaling, fluctuations.

DOI: 10.1103/PhysRevLett.126.057801

The natural or artificial production of high-performance polymeric materials requires precise control over flow-induced crystallization. This phenomenon involves in turn a highly nontrivial interdependence between the molecular level of bond-orientation-dependent nucleation, and the macroscopic level, where the temperature-dependent rheology generates stretch of entire chain segments [1–5]. Remarkably, nature has found a way to control robustly the flow-induced self-assembly of silk from an intrinsically disordered state (a solution of random-walk polymers) prior to forming high-performance fibers under flow at ambient conditions [6–14]. Key to achieving the final properties is that silk is processed in semidilute aqueous conditions [10], where nucleation can be induced through the stretch-induced disruption of the solvation layer [15]. How sufficient polymer stretch can be achieved in a limited time under modest flow conditions [9,16] has so far remained unexplained. An important clue has been the observation of *strain hardening* [9,16], which in *B. mori* silk [16] turned out to be triggered by a small number of calcium bridges [14,17] that act as "sticky" reversible intermolecular crosslinks akin to those in synthetic "sticky polymers" [18–26]. For this class of molecules, a molecular understanding of the nonlinear rheology and crystallization of sticky polymers has so far relied on computationally expensive (albeit coarse grained to some degree) molecular dynamics simulations [5,27–32]. Simpler molecular models coarse grained at the level of entanglements, but able to capture the vital slow processes, remain absent.

In the present work, we address this need by following the central idea by de Gennes and Edwards of replacing the many-chain problem with a single chain in a tubelike confinement imposed by its environment of entanglements [33,34], and solve the Brownian dynamics of the chain in 1D [35]. This approach is simple yet powerful, and has led to the development of widely applied finite-element solvers [36–39], a physical explanation for the (apparent) 3.4 power dependence of the relaxation time of polymer melts on the molecular weight [40], and a comprehensive understanding of the rich nonlinear rheology of (bimodal) polymer blends [41,42]. In the spirit of other theory and modeling work on associating polymers [38], in this Letter we add a description for the stochastic attachment and detachment of associating monomers to the tubular environment developed for full nonlinear flows. The model shares some structural similarities with early "transient network" approaches to polymer melt and solution rheology [43], also demonstrating a hitherto unrecognized feature of those models.

The starting point of our contribution is to consider a chain consisting of N Kuhn segments with length b, and Z_e entanglements [hence, with tube diameter $a = b(N/Z_e)^{1/2}$]. The configuration of the chain is given by the spatial coordinates R_i of monomers $i = 1, \ldots, N$ along the curvilinear direction along the tube, which evolve with time according to the Langevin equation [35,40,41]

$$\zeta \frac{\partial R_i}{\partial t} = \left(\frac{3k_B T}{b^2} \frac{\partial^2 R_i}{\partial i^2} + f_i \right)(1 - p_i) + \dot{\varepsilon} \zeta R_i, \qquad (1)$$

with $\partial R/\partial i = aZ_e/N$ at $i = 1$ and at $i = N$, ζ the monomeric friction, $k_B T$ the thermal energy, and f_i a stochastic force given by the equipartition theorem

$$\langle f_i(t) \rangle = 0; \quad \langle f_i(t) f_{i'}(t') \rangle = 2k_B T \zeta \delta(i' - i) \delta(t' - t). \qquad (2)$$

In the absence of stickers, this equation predicts the Rouse diffusivity [34]

$$D_R = \frac{a^2}{3\pi^2 \tau_e Z_e} = \frac{k_B T}{\zeta N} \tag{3}$$

and the variance of quiescent contour-length fluctuations $\langle |R_N - R_1|^2 \rangle = a Z_e/3$. The strain rate $\dot{\varepsilon}$ is in one spatial dimension equivalent to the strain rate in the GLaMM model [41].

To model the binding and unbinding of monomers to the environment, we introduce a stochastic state variable $p_i(t)$, which takes values of either zero or unity for each monomer i, which represents the "open" and "closed" states of a monomer, respectively. An open monomer i is unbound and is free to diffuse and respond to the drag exerted by the flow field, as well as to relax stress in adjoining segments. If this monomer represents a sticker, it may close through either association or bond-swapping events [44,45]. The effective closing rate $k_{i,\mathrm{close}}$ sets the probability $1 - \exp(-k_{i,\mathrm{close}}\Delta t) = k_{i,\mathrm{close}}\Delta t + \mathcal{O}(\Delta t^2)$ of closing after a time interval Δt for small Δt. In every time step of our simulations a random number $r \in [0, 1]$ is drawn and the sticker is closed if $r < k_{i,\mathrm{close}}\Delta t \ll 1$ [37] and is now kinetically trapped by its environment and is unable to diffuse or to respond to local stress in the polymer. Hence, the closed sticker advects with the background flow. The sticker may reopen according to the same recipe as above, but now with an opening rate $k_{i,\mathrm{open}}$.

In principle, for copolymers or polymers with intramolecular (secondary) structures, each monomer can have different opening and closing rates. Here, we consider polymers with N Kuhn segments of which $Z_s \ll N$ are chemically identical stickers. The nonsticky segments are always open, while the stickers may switch between open and closed states with rates k_{close} and k_{open}. The opening rate is approximately constant if the force within the chain does not significantly decrease the activation energy for sticker dissociation. For instance, for silk the activation barrier is $8k_BT \approx 24$ pNnm [14] and instantaneous bond dissociation over 0.1 nm requires approximately a force of 240 pN. To produce this force f, chain alignment alone is not enough (the tube model gives an entanglement-generated chain tension of $3k_BT/a$) while by Gaussian stretching and disentangling [46]

$$f = 3k_BT(R_s - R_{s,0})/R_{s,0}^2, \tag{4}$$

it would be required to stretch the quiescent distance between stickers $R_{s,0} \approx 9$ nm [47] to $R_s \approx 1800$ nm (using the sticker rather than the entanglement strand tacitly assumes $Z_s \gtrsim Z_e$, and if entanglements persist at these extreme stretches the critical stretch for sticker detachment is reduced by $\sqrt{Z_e}$). On the other hand, full extension of the substrand between stickers is already achieved at $R_s \approx 200$ nm [48]: in practice, therefore, it seems likely the destabilization of the stickers by the chain tension occurs, for silk, in the same regime where finite-extensibility effects emerge [49]. By approximating k_{open} as a constant, it can be related to the rheological sticker lifetime as $\tau_s = k_{\mathrm{open}}^{-1}$ [14,19,26,28–31], and the closing rate is given by $k_{\mathrm{close}} = k_{\mathrm{open}} p/(1-p)$, with p the time- or ensemble-averaged fraction of closed stickers. Hence, we will treat p and τ_s as free model parameters [19].

We have benchmarked our model in the absence of flow using the Likhtman-McLeish model for linear nonsticky polymers [35] (this linear rheological response is not shown here) and using the sticky-Rouse (SR) diffusivity $D_{\mathrm{SR}} = D_{\mathrm{SR}}(Z_e, \tau_e, Z_s, \tau_s, p)$ as calculated by Leibler *et al.* [19] (see the inset of Fig. 1). For the nonlinear dynamics of sticky polymers, so far no comparisons between analytical predictions with simulations or experiments have been reported. The first strategy to address this is to evaluate how well a Doi-Edwards-Marrucci-Grizzuti (DEMG)-type single-mode approximation performs [49], with chain friction renormalized by averaging over the stochastic sticker dynamics:

$$\frac{d\lambda}{dt} = \dot{\varepsilon}\lambda + \frac{1}{\tau_{\mathrm{SR}}}(1 - \lambda), \tag{5}$$

where the stretch ratio $\lambda \equiv (R_N - R_1)/Z_e$ is presumed to be uniform over the backbone of the chain. The extension rate

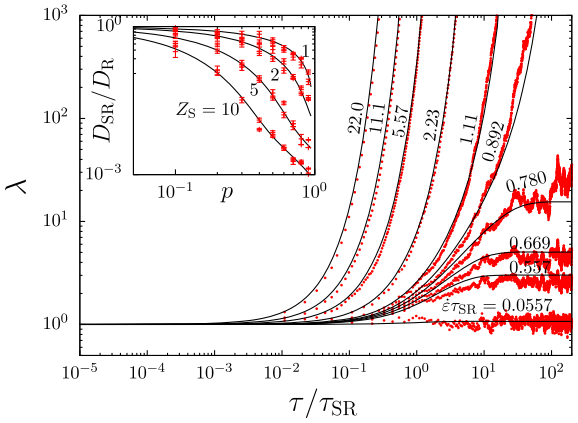

FIG. 1. Comparison between the stretch ratio λ of a sticky polymer ($Z_e = Z_s = 10$, $\tau_s = 10^4\tau_e$, $p = 0.95$, $Z_s = 10$) against time t in units of the sticky Rouse time τ_{SR} at a range of flow rates from $\dot{\varepsilon} = 0.056\tau_{\mathrm{SR}}^{-1}$ to $22.3\tau_{\mathrm{SR}}^{-1}$ in logarithmic steps. The sticky Rouse time is $\tau_{\mathrm{SR}} = [D_R/D_{\mathrm{SR}}]\tau_R$ with D_R the bare Rouse diffusivity, $\tau_R = \tau_e Z_e^2$ the bare Rouse time, and D_{SR} the sticky diffusivity (see inset). In the main panel, the symbols are obtained by averaging over five Brownian dynamics simulations with different random number seeds; the lines represent the single-mode model in Eq. (5). The inset shows consistence of the simulated sticky-Rouse diffusivity (symbols; averaged over 25 random number seeds) with the sticky-reptation model (lines) of Leibler *et al.* [19].

is proportional to the stretch ratio itself. The retraction rate is determined by $(1-\lambda)$ (in the absence of flow, $\lambda = 1$ at steady state) and by the sticky-Rouse time $\tau_{SR} \equiv [D_R/D_{SR}]\tau_S$. In the main graph of Fig. 1, we present a comparison between this simple approximation and our simulations (the approximations inherent in the DEMG require that the simulation time be divided by a factor 1.2 to result in the close agreement shown). This confirms that the intuitive "sticky Weissenberg number" for the stretch transition is $\mathrm{Wi} = \dot{\varepsilon}\tau_{SR}$. For $\mathrm{Wi} > 1$ an exponential runaway stretch emerges as expected. In contrast to nonsticky polymers, however, we will argue that the stress and fluctuation in stretch may diverge *below* this stretch transition when the preaveraging approximation inherent in DEMG is avoided.

While nonsticky polymers in steady state show a Gaussian stretch distribution with a width that is determined by the (effective) number of entanglements, we have observed rather large stretch fluctuations for the sticky polymer at extension rates of the order of, but below, the critical value. Indeed, the symbols in Fig. 1 are averaged over five simulations for a chain with ten stickers which are on average closed a fraction $p = 0.95$ of time. For simulations with $p < 0.9$ these fluctuations become much larger and difficult to distinguish graphically. Indeed, while the mean stretch is finite, the fluctuations in stretch diverge above a certain flow rate *below* the stretch transition.

For three of the flow rates shown in Fig. 1 we have plotted the stretch distribution $P(\lambda)$ in Fig. 2. For small

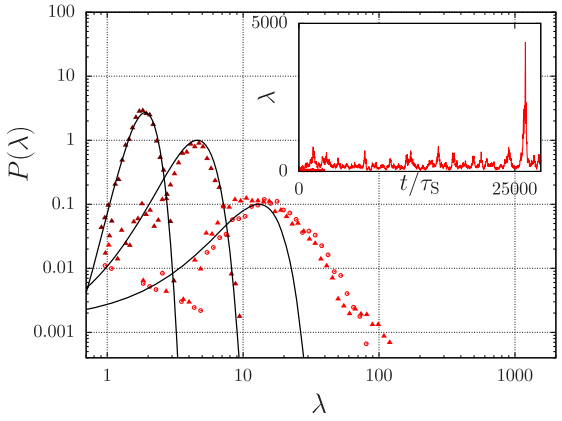

FIG. 2. The steady-state probability distribution $P(\lambda)$ is plotted against the stretch ratio λ. The symbols are obtained from the steady-state simulations of Fig. 1 at the flow rates ($\dot{\varepsilon}\tau_{SR} = 0.446$, 0.668, and 0.780); the curves are Gaussian fits. For an increasing flow rate, the high-stretch tail is no longer Gaussian but becomes a power law $P(\lambda) \propto \lambda^{-\nu}$. The inset shows the stretch ratio against time for $\dot{\varepsilon}\tau_{SR} = 0.780$ and visualizes how this distribution includes "rare events" of enormous chain stretch. For a sufficiently large flow rate, ν decreases. If $\nu > 2$, the mean value of λ is finite (as it should in steady state); however, if also $\nu \leq 3$, the fluctuations in stretch, characterized by the expectation value of λ^2, diverge.

flow rates, the stretch distribution is Gaussian, $\ln P(\lambda) \propto (1-\lambda)^2$ (solid curves), as in the quiescent state. However, for increased flow rates deviations emerge in the high-λ tail of the distribution. Importantly, the polymer stretch may resemble the mean stretch for long times compared to the sticky-Rouse time, and only in "rare events" the stickers may remain closed sufficiently long for the stretch to reach deep into the tail of the distribution (see inset).

In the following, we will explore the problem analytically using a "sticky dumbbell model" to explore and clarify the underlying causes of the power law tail in the stretch distribution, and explore how it can be tuned by the flow rate. This minimal model that captures the essential physics is equivalent to a single polymer strand either attached to the bulk deformation at both ends (the closed state) or free to relax (the open state). The rate by which the polymer switches between the two states is given by the usual opening and closing rates. We can now address the development of stretch under extensional flow through a pair of coupled partial differential equations for the time-dependent stretch distributions $P_o(t,\lambda)$ and $P_c(t,\lambda)$ for each state using the master equation

$$\frac{\partial P_c}{\partial t} = -\frac{\partial}{\partial \lambda}[P_c \dot{\varepsilon}\lambda] - k_{\mathrm{open}} P_c - k_{\mathrm{close}} P_o,$$
$$\frac{\partial P_o}{\partial t} = -\frac{\partial}{\partial \lambda}\left[P_o\left(\dot{\varepsilon}\lambda + \frac{1-\lambda}{\tau_R}\right)\right] + k_{\mathrm{open}} P_c - k_{\mathrm{close}} P_o. \quad (6)$$

Note that this evolution equation invokes a single-mode approximation and ignores thermal fluctuations: the stretch distribution emerges from the coupling between a closed state in which the polymer is stretched and the open state in which it can retract. Under strong flow conditions, the effective driving noise is completely dominated by the stochastic state switching, with thermal noise negligible.

We calculate the steady-state stretch distribution at strong stretch by setting the left-hand side of Eq. (6) to zero and taking $\lambda \gg 1$. The result can be solved analytically since in these conditions the differential system becomes homogeneous. We therefore find the power law relation

$$P(\lambda) \propto \lambda^{-\nu}, \quad (7)$$

with the exponent given in terms of the three dimensionless parameters of the system, p, $\dot{\varepsilon}\tau_R$, τ_R/τ_s by

$$\nu = 1 + \frac{1}{(1-\dot{\varepsilon}\tau_R)}\frac{p}{(1-p)}\frac{\tau_R}{\tau_s} - \frac{1}{\dot{\varepsilon}\tau_s}. \quad (8)$$

We compare this power law to our sticky dumbbell simulations in Fig. 3. In passing, we note that this model also provides an example of one of a family of driven, stochastic, systems together referred to as "multifractals" [50] in which a divergent and scaling structure of fluctuations arises, not just at a single critical point, but within a

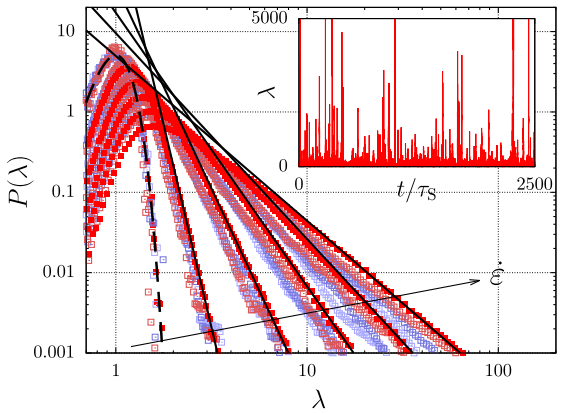

FIG. 3. The power law stretch distribution, $P(\lambda) \propto \lambda^{-\nu}$ for large λ, observed in Fig. 2 is replicated analytically in a sticky dumbbell model for a sticky polymer ($Z_e = 10$, $p = 0.9$, $\tau_s = 1000\tau_e$), which has two stickers near the end of the chain that are simultaneously either open or closed (lines). The dashed curve is the Gaussian stretch distribution under quiescent conditions. In linear steps, the flow rate is increased up to $\dot{\varepsilon}\tau_R = 0.05$. The symbols are obtained in simulations with 2, 6, 12, and 36 beads (from red to light blue). For small flow rates, where $\nu < 3$, the simulated power law tails of $P(\lambda)$ (symbols) are in agreement with Eq. (8). The inset shows the transient behavior of the simulation with $\dot{\varepsilon}\tau_R = 0.05$.

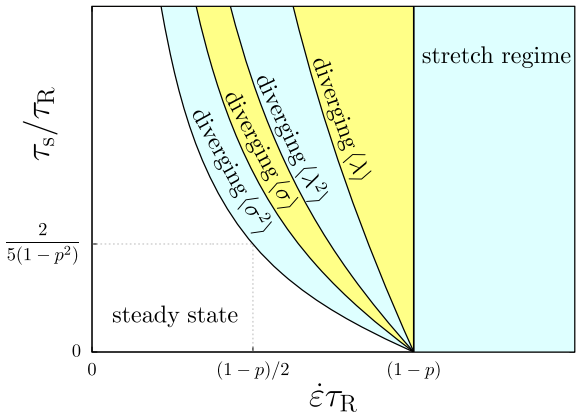

FIG. 4. State diagram of a sticky dumbbell. For a short sticker lifetime, polymer stretching takes place if the Weissenberg number $(1-p)\dot{\varepsilon}\tau_R$ is larger than unity. p is the time-averaged fraction of closed stickers and τ_R is the bare Rouse time. For a finite sticker lifetime, the mean and the variance of the stress σ and the stretch λ diverge in different regimes. The curves are given by Eq. (8) for $\nu = 2, 3, 4, 6$ as discussed in the main text.

large region of state space, and with a universal critical exponent replaced by a family, dependent on the degree of forcing.

For sufficiently small flow rates, we find a reasonable agreement between our multibead simulations and the analytical approximation for the simple sticky dumbbell (under these conditions, $\nu > 3$). While the simulation for chains with just two beads (i.e., with a single Rouse mode) agrees well with the approximate theory, the higher Rouse modes in the multibead chain provide an additional relaxation mechanism for the retraction of the chain ends alike contour-length fluctuations. Hence, the single-mode approximation slightly overestimates the width of the stretch distribution of a real chain (i.e., a multibead chain). The discrepancy between the single-mode and multibead chain becomes apparent if the flow rates are high for the exponent ν to approach or go beyond a value 3 [this occurs at $(1-p)\dot{\varepsilon}\tau_R \approx \tau_R/(2\tau_s)$]. This is not a coincidence: if $\nu = 3$ the magnitude of the fluctuations diverge, $\langle\lambda^2\rangle \to \infty$. Although the fluctuations diverge for $\nu = 3$, the mean $\langle\lambda\rangle$ remains finite as long as $\nu \leq 2$ [the equality holds approximately when $(1-p)\dot{\varepsilon}\tau_R \approx \tau_R/\tau_s$]. For even larger flow rates, i.e., for $\nu \leq 1$ [at $(1-p)\dot{\varepsilon}\tau_s = 1$] the stretch distribution can no longer be normalized and true runaway stretch emerges. These various regimes are displayed in Fig. 4 in terms of the dimensionless parameters of the system. Note that the stress is $\sigma \propto (1-\lambda)^2$ and the tail of the stress distribution is $P(\sigma) \propto \lambda^{-\nu/2}$: the mean stress diverges for $\nu \leq 4$ and its variance diverges for $\nu \leq 6$.

The single-mode dumbbell model clarifies the route through which the divergent fluctuations arise. Crucially, when a stretched strand is freed from the network, it may not relax entirely before reattachment (this effect is ignored in classical treatments of transient network models, which in consequence overlook the strong stochastic fluctuations they physically imply). Such continuous interchange between convecting and relaxing strands, together with the occurrence of longer-than-average attachment times for some segments, allow the exploration of very large chain stretches in steady state.

To illustrate the potential consequences of this effect, we consider nucleation rates in steady-state extensional flow, assuming that polymer crystal phase may nucleate around chains beyond a critical stretch ratio λ_* [1]. Assuming that the chain is relaxed prior to sticker closing at time $t = 0$, its stretch ratio develops as $\lambda(t) = \exp(\dot{\varepsilon}t)$ until it opens at a time τ_{open}. This time is drawn from the probability distribution $p(\tau_{\text{open}}) = \tau_s^{-1}\exp(-\tau_{\text{open}}/\tau_s)$, so the probability that the critical stretch is reached is $p_* = \lambda_*^{-1/\dot{\varepsilon}\tau_s}$. The probability that λ_* is not reached after n attempts is $(1-p_*)^n$, and therefore the expected number of attempts needed is

$$\langle n\rangle = \frac{\sum_{n=1}^{\infty} n(1-p_*)^n}{\sum_{n=1}^{\infty}(1-p_*)^n} = \lambda_*^{1/(\dot{\varepsilon}\tau_s)}. \tag{9}$$

An attempt occurs, on average, after time intervals $1/k_{\text{open}} + 1/k_{\text{close}} = \tau_s/p$. If the number density of chains is ρ, then combining these results gives an extension-rate-dependent nucleation rate per volume $J = [\rho p/\tau_s]\lambda_*^{-1/(\dot{\varepsilon}\tau_s)}$. We expect that the form

$$\ln J = A - \frac{B}{\dot{\varepsilon}\tau_s}, \tag{10}$$

with A and B flow-independent coefficients, carries over to the multisticker chain provided that the substrand between stickers is sufficiently long and τ_s can be treated as a constant [see our discussion on Eq. (4)]. This constitutes a first prediction for the rate of flow-induced crystallization of associating polymers in steady-state extensional flow, which along with the prediction of strong stretch fluctuations will help the interpretation of the (noisy) nonlinear rheology of silk [9,16], e.g., using confocal microscopy [51] and controlled variations of ionic content in the solution [52], and thereby aid the development of its synthetic counterparts [15].

In conclusion, we have numerically solved the 1D stochastic Langevin equation of an aligned entangled sticky polymer in an effective medium and in extensional flow. We show that this computationally inexpensive simulation method captures the combined polymer physics of reptation, contour-length-fluctuations and response in extensional flow, associating stickers. Crucially, it does not preaverage any fluctuations in chain stretch, and predicts that in steady-state flow a small fraction of chains (rather than all of them) stretches to a large extent: this seems a promising energy-efficient strategy to trigger the flow-induced crystallization of polymers. For simulations that can be quantitatively compared to experiment, it will be necessary to include a description for finite chain extensibility, and to account for the effect of chain stretch reducing the sticker binding energy and lifetime, although we expect the power law tails in the stretch distribution found here to survive with corresponding cutoffs.

This research was funded by the Engineering and Physical Sciences Research Council [Grant No. EPSRC (EP/N031431/1)]. Jorge Ramírez is thanked for sharing Alexei Likhtman's Brownian dynamics code and Richard Graham is thanked for sharing his GLaMM code; both codes helped us to benchmark our simulation software. Chris Holland and Pete Laity are thanked for useful and encouraging discussions.

*charley.schaefer@york.ac.uk

[1] R. S. Graham and P. D. Olmsted, Phys. Rev. Lett. **103**, 115702 (2009).
[2] E. M. Troise, H. J. M. Caelers, and G. W. M. Peters, Macromolecules **50**, 3868 (2017).
[3] D. A. Nicholson and G. C. Rutledge, J. Rheol. **63**, 465 (2019).
[4] S. Moghadamand, I. S. Dalal, and R. G. Larson, Macromolecules **52**, 1296 (2019).
[5] D. J. Read, C. McIlroy, C. Das, O. G. Harlen, and R. S. Graham, Phys. Rev. Lett. **124**, 147802 (2020).
[6] T. Asakura, H. Suzuki, and Y. Watanabe, Macromolecules **16**, 1024 (1983).
[7] T. Asakura, Y. Watanabe, A. Uchida, and H. Minagawa, Macromolecules **17**, 1075 (1984).
[8] C. Zhao and T. Asakura, Prog. Nucl. Magn. Reson. Spectrosc. **39**, 301 (2001).
[9] N. Kojić, J. Bico, C. Clasen, and G. H. McKinley, J. Exp. Biol. **209**, 4355 (2006).
[10] C. Holland, F. Vollrath, A. J. Ryan, and O. O. Mykhaylyk, Adv. Mater. **24**, 105 (2012).
[11] T. Asakura, K. Okushita, and M. P. Williamson, Macromolecules **48**, 2345 (2015).
[12] P. R. Laity, S. E. Gilks, and C. Holland, Polymer **67**, 28 (2015).
[13] P. R. Laity and C. Holland, Biomacromolecules **17**, 2662 (2016).
[14] C. Schaefer, P. R. Laity, C. Holland, and T. C. B. McLeish, Macromolecules **53**, 2669 (2020).
[15] G. J. Dunderdale, S. J. Davidson, A. J. Ryan, and O. O. Mykhaylyk, Nat. Commun. **11**, 3372 (2020).
[16] A. Koeppel, P. R. Laity, and C. Holland, Soft Matter **14**, 8838 (2018).
[17] P. R. Laity, E. Baldwin, and C. Holland, Macromol. Biosci. **19**, 1800188 (2018).
[18] O. Kramer, *Biological and Synthetic Polymer Networks* (Elsevier Applied Science, New York, 1988).
[19] L. Leibler, M. Rubinstein, and R. H. Colby, Macromolecules **24**, 4701 (1991).
[20] R. A. Weiss, J. J. Fitzgerald, and D. Kim, Macromolecules **24**, 1071 (1991).
[21] T. Annable, R. Buscall, R. Ettelaie, and D. Whittlestone, J. Rheol. **37**, 695 (1993).
[22] R. H. Colby, X. Zheng, M. H. Rafailovich, J. Sokolov, D. G. Peiffer, S. A. Schwarz, Y. Strzhemechny, and D. Nguyen, Phys. Rev. Lett. **81**, 3876 (1998).
[23] R. A. Weiss and W. C. Yu, Macromolecules **40**, 3640 (2007).
[24] S. Seiffert and J. Sprakel, Chem. Soc. Rev. **41**, 909 (2012).
[25] S. Hackelbusch, T. Rossow, P. van Assenbergh, and S. Seiffert, Macromolecules **46**, 6273 (2013).
[26] Z. Zhang, Q. Chen, and R. H. Colby, Soft Matter **14**, 2961 (2018).
[27] T. Yamane, K. Umemura, Y. Nakazawa, and T. Asakura, Macromolecules **36**, 6766 (2003).
[28] Q. Chen, Z. Zhang, and R. H. Colby, J. Rheol. **60**, 1031 (2016).
[29] T. Tomkovic and S. G. Hatzikiriakos, J. Rheol. **62**, 1319 (2018).
[30] T. Tomkovic, E. Mitsoulis, and S. G. Hatzikiriakos, Phys. Fluids **31**, 033102 (2019).
[31] M. Zuliki, S. Zhang, K. Nyamajaro, T. Tomkovic, and S. G. Hatzikiriakos, Phys. Fluids **32**, 023104 (2020).
[32] G. Cui, V. A. H. Boudara, Q. Huang, G. P. Baeza, A. J. Wilson, O. Hassager, D. J. Read, and J. Mattsson, J. Rheol. **62**, 1155 (2018).
[33] P. G. de Gennes, J. Chem. Phys. **55**, 572 (1971).
[34] M. Doi and S. F. Edwards, *The Theory of Polymer Dynamics* (Clarendon, Oxford, 1986).
[35] A. E. Likhtman and T. C. B. McLeish, Macromolecules **35**, 6332 (2002).

[36] A. E. Likhtman and R. S. Graham, J. Non-Newtonian Fluid Mech. **114**, 1 (2003).
[37] V. A. H. Boudara and D. J. Read, J. Rheol. **61**, 339 (2017).
[38] V. A. H. Boudara, D. J. Read, and J. Ramírez, J. Rheol. **64**, 709 (2020).
[39] M. W. Collis, A. K. Lele, M. R. Mackley, R. S. Graham, D. J. Groves, A. E. Likhtman, T. M. Nicholsona, O. G. Harlen, T. C. B. McLeish, L. R. Hutchings, C. M. Fernyhough, and R. N. Young, J. Rheol. **49**, 501 (2005).
[40] M. Doi, J. Polym. Sci. Polym. Phys. Ed. **21**, 667 (1983).
[41] R. S. Graham, A. E. Likhtman, T. C. B. McLeish, and S. T. Milner, J. Rheol. **47**, 1171 (2003).
[42] D. Auhl, P. Chambon, T. C. B. McLeish, and D. J. Read, Phys. Rev. Lett. **103**, 136001 (2009).
[43] M. S. Green and A. V. Tobolsky, J. Chem. Phys. **14**, 80 (1946).
[44] F. Smallenburg, L. Leibler, and F. Sciortino, Phys. Rev. Lett. **111**, 188002 (2013).
[45] S. Ciarella, F. Sciortino, and W. G. Ellenbroek, Phys. Rev. Lett. **121**, 058003 (2018).
[46] M. Rubinstein and R. H. Colby, *Polymer Physics*, 4th ed. (Oxford University Press, Oxford, 2003).
[47] From the end-to-end distance $R_e = Z_s^{1/2} R_s$ with $Z_s = 5$–10 [14] and $R_e = \sqrt{6} R_g$ with $R_g = 10$ nm [13], we have $R_{s,0} = 7.9$–11 nm.
[48] The step size of an amino acid is 0.36 nm and silk has substrands of 550 amino acids between stickers [13,14].
[49] J. M. Dealy, D. J. Read, and R. G. Larson, *Structure and Rheology of Molten Polymers* (Hanser, Munich, 2018).
[50] D. Harte, *Multifractals* (Chapman and Hall/CRC, New York, 2001).
[51] C. Holland, J. Urbach, and D. L. Blair, Soft Matter **8**, 2590 (2012).
[52] A. Koeppel, P. R. Laity, and C. Holland, Acta Biomater. **117**, 204 (2020).